Supporting Information

Khandekar et al. 10.1073/pnas.1717776115

SI Experimental Procedures

Reagents. Rosiglitazone and pioglitazone were purchased from Sigma. SR1664, SR1824, SR10171, and MRL-24 were synthesized at Scripps Florida, as previously described (1, 2). Doxorubicin, carboplatin, taxol, and etoposide for cell culture experiments were purchased from Sigma. Pharmaceutical grade carboplatin for animal experiments was purchased from Patterson Veterinary.

Antibodies. Antibodies were obtained from Cell Signaling unless otherwise specified. The PPARγ IP experiments were performed using E-8 antibody from Santa Cruz. The phospho-specific antibody to pS273 PPARγ has previously been described (3).

Cell Culture. To generate immortalized fibroblasts, interscapular brown adipose stromal vascular fraction was obtained from 4-wk-old mice with the following genotypes: $Pparg^{wt/wt}$ or $Pparg^{S273A/S273A}$. Interscapular brown adipose was dissected, washed in PBS, minced, and digested for 45 min at 37 °C in PBS containing 1.5 mg/mL collagenase B (Roche), 123 mM NaCl, 5 mM KCl, 1.3 mM $CaCl_2$, 5 mM glucose, 100 mM Hepes, and 4% essentially fatty acid-free BSA. Tissue suspension was filtered through a 40-μm cell strainer and centrifuged at 600 × *g* for 5 min to pellet the fibroblastic cells. The cell pellet was resuspended in DMEM+ 10% FBS and plated. After 3 d of culture, a fibroblastic culture was obtained. These cells were then infected with lentivirus containing SV40 (abm). Cells were verified for infection by RT-PCR for SV40 viral antigens. These cells were maintained in DMEM+10% FBS.

For lentiviral experiments, 293T cells were transfected with Fugene 6 (Roche) with viral vectors and supernatants harvested after 48 h. shRNA and scramble constructs were obtained from the Dana Farber Cancer Institute RNA Interference Screening Facility. Cells were infected for 24 h, and analyzed 24 h after infection was completed.

RT-PCR. RNA was extracted from cultured cells or frozen tissue samples using TRIzol (Invitrogen), purified with Qiagen RNeasy minicolumns and reverse-transcribed using a High Capacity cDNA Reverse Transcription kit (Applied Biosystems). Resulting cDNA was analyzed by qRT-PCR. Briefly, 25 ng of cDNA and 150 nmol of each primer were mixed with SYBR GreenER PCR Master Mix (Invitrogen). Reactions were performed in 384-well format using an ABI PRISM 7900HT instrument (Applied Biosystems). Relative mRNA levels were calculated using the comparative CT method normalized to TATA binding protein mRNA.

IP and Western Blotting. For IP, crude nuclear extracts were prepared from confluent cells grown on 15-cm plates. Cells were washed with PBS, scraped, and pelleted by centrifugation at 4°. Cells were resuspended in buffer (20 mM Tris, 100 mM NaCl, 300 mM Sucrose, 3 mM $MgCl_2$) and incubated on ice for 10 min. Cells were centrifuged at 900 × *g* at 4°. The pellet was resuspended in 187 μL of nuclear extraction buffer (20 mM Tris, 100 mM NaCl, 2 mM EDTA) and the volume was measured. A volume of 5 M NaCl was added to the solution to bring the total concentration of NaCl to 0.42 M, and the solution was pipetted vigorously. Pellets were incubated on ice for 30 min with occasional mixing, and then spun at maximum speed for 20 min at 4°. Protein was quantified for SDS/PAGE using a BCA assay (Pierce). For IP, 1 g of nuclear extract protein was diluted in buffer containing 50 mM Tris, 1% Igepal CA-360, 10% glycerol, and the final concentration of NaCl was adjusted to 150 mM. PPARγ was immunoprecipitated with antibody overnight, and antigen/antibody complexes were collected using Dynabeads Protein G (ThermoFisher) and a magnetic rack. Beads were washed five times with the IP buffer, and elution was performed using NuPage LDS buffer with 2.5% β-mercaptoethanol and boiling for 5 min. Samples were run on NuPage SDS gells with Mops buffer and Western blotting performed as described previously (3). For conventional Western blotting, samples were collected and lysed in RIPA buffer and run on NuPage SDS gels, as described above.

Animal Experiments. All animal experiments were approved by the Institutional Animal Care and Use Committee of the Beth Israel Deaconess Medical Center. Mice (*Mus musculus*) were maintained in 12-h light/dark cycles (6:00 AM–6:00 PM) at 24 °C. Nude mice were purchased from Taconic and maintained in autoclaved cages with irradiated diet that had also been autoclaved. Six- to 10-wk-old male mice were used for xenograft experiments. Preliminary data suggested groups of 8–10 mice were appropriate to achieve sufficient power to detect a difference between DMSO treatment and treatment with SR1664. Xenografts were generated by injecting 5×10^6 cells in DMEM media into the flank. Tumor dimensions were measured twice weekly using tumor calipers and converted to volume using the formula $V = (\pi \times \text{length}) \times (\text{width}^2/6)$. Treatment was started once tumors measured 50–75 mm^3 were present on the flank. Animals were randomly assigned to treatment groups of: vehicle, vehicle + carboplatin (50 mg/kg, Monday, Wednesday, and Friday), pioglitazone (7.5 mg/kg, twice a day) + carboplatin, SR1664 (20 mg/kg), and SR1664 + carboplatin. Mice were weighed daily for dosing. Treatment drugs were dissolved in vehicle containing DMSO, Cremophor EL, and sterile saline. Drugs were delivered via intraperitoneal injection twice a day. Carboplatin or sterile saline was delivered via intraperitoneal injection on Monday, Wednesday, and Friday.

Microarray Analysis. RNA was harvested and hybridization performed by the Dana Farber Cancer Institute Molecular Biology Core Facilities. Affymetrix Mouse Gene 2.0 ST chips were used. Data were analyzed using Affymetrix Expression Console software and Transcriptome Analysis Console. A gene set was defined as genes that were >threefold up-regulated with a significant *P* value (false-discovery rate $P < 0.05$). These were validated in separate qPCR experiments using cDNA from fibroblasts. A refined gene set was generated from these genes with exclusion of genes that were not expressed across a wide variety of cells and tissues. GSEA was performed as described (4) using the Hallmark Gene sets defined in the MSigDB.

For analysis of clinical data, raw Affymetrix data were downloaded from the Gene Expression Omnibus (https://www.ncbi.nlm.nih.gov/geo) for the NIH Director's Challenge's study (5) and the UT Lung Spore Cohort (6), along with the clinical data. Patients who did not receive adjuvant chemotherapy were excluded. Affymetrix data were normalized using RMA in R (RStudio 1.0.143). The probe IDs associated with the genes in the gene signature were identified. If any genes were not represented in the array used, it was discarded. The median gene expression of each probe ID was calculated. To generate a classifying statistic, for genes that were down-regulated by S273A mutation, patients with gene expression less than the median

were assigned a value of 1, while those who had a gene expression greater than the median had a value of 0. Conversely, for genes that were up-regulated by S273A mutation, patients whose gene expression was greater than the median were assigned a value of 1 and those whose value was less than the median were 0. These values were summed and the median value of the classifier statistic was calculated. Patients whose classifying statistic was greater than the median were defined as having a positive signature, while those less than the median were defined as having a negative signature. The association of signature classification with survival was analyzed using the survfit function, and a Kaplan–Meier plot was generated using ggplot2 in RStudio. Significance was calculated using log-rank test using the survdiff function.

As an alternative approach, we used the online tool KMplot (kmplot.com/analysis/index.php?p=background) to analyze data for breast cancer (7). We restricted our analysis to patients with ER^-/PR^- cancers who received adjuvant chemotherapy and used their multigene classifier with the down-regulated genes weighted as −1 and the up-regulated genes weighted as 1. Patients were split at the median, and recurrence-free survival was analyzed. A similar analysis was carried out excluding patients who received systemic chemotherapy. Analysis of lung cancer patients for overall survival was undertaken with a similar approach.

Microscopy. Tumors or lungs were removed from animals and fixed with 4% paraformaldehyde followed by dehydration in 70% ethanol before embedding. Tissues were embedded in paraffin by the Rodent Histopathology Core at Harvard Medical School. Immunohistochemistry was performed as described previously (8). TUNEL staining was performed using the Apoptag Peroxidase in Situ Apoptosis Detection Kit (EMD Millipore) per the manufacturer's instructions. Images were acquired containing the entire tissue section, and analyzed using the Aperio Imagescope Software, which was performed by the Dana Farber/Harvard Cancer Center Research Pathology Core.

Statistics. Student's test was used for single comparisons of mean values. Error bars represent ± SEM except when otherwise specified. Two-way ANOVA was used to compare multiple groups. A chi-square test was used to compare gene expression changes in the gene set. An asterisk (*) indicates $P < 0.05$ except when specified.

1. Choi JH, et al. (2011) Antidiabetic actions of a non-agonist PPARγ ligand blocking Cdk5-mediated phosphorylation. *Nature* 477:477–481.
2. Stechschulte LA, et al. (2016) PPARG post-translational modifications regulate bone formation and bone resorption. *EBioMedicine* 10:174–184.
3. Choi JH, et al. (2010) Anti-diabetic drugs inhibit obesity-linked phosphorylation of PPARgamma by Cdk5. *Nature* 466:451–456.
4. Mootha VK, et al. (2003) PGC-1alpha-responsive genes involved in oxidative phosphorylation are coordinately downregulated in human diabetes. *Nat Genet* 34: 267–273.
5. Shedden K, et al.; Director's Challenge Consortium for the Molecular Classification of Lung Adenocarcinoma (2008) Gene expression-based survival prediction in lung adenocarcinoma: a multi-site, blinded validation study. *Nat Med* 14:822–827.
6. Tang H, et al. (2013) A 12-gene set predicts survival benefits from adjuvant chemotherapy in non-small cell lung cancer patients. *Clin Cancer Res* 19:1577–1586.
7. Győrffy B, et al. (2010) An online survival analysis tool to rapidly assess the effect of 22,277 genes on breast cancer prognosis using microarray data of 1,809 patients. *Breast Cancer Res Treat* 123:725–731.
8. Lo JC, et al. (2014) Adipsin is an adipokine that improves β cell function in diabetes. *Cell* 158:41–53.

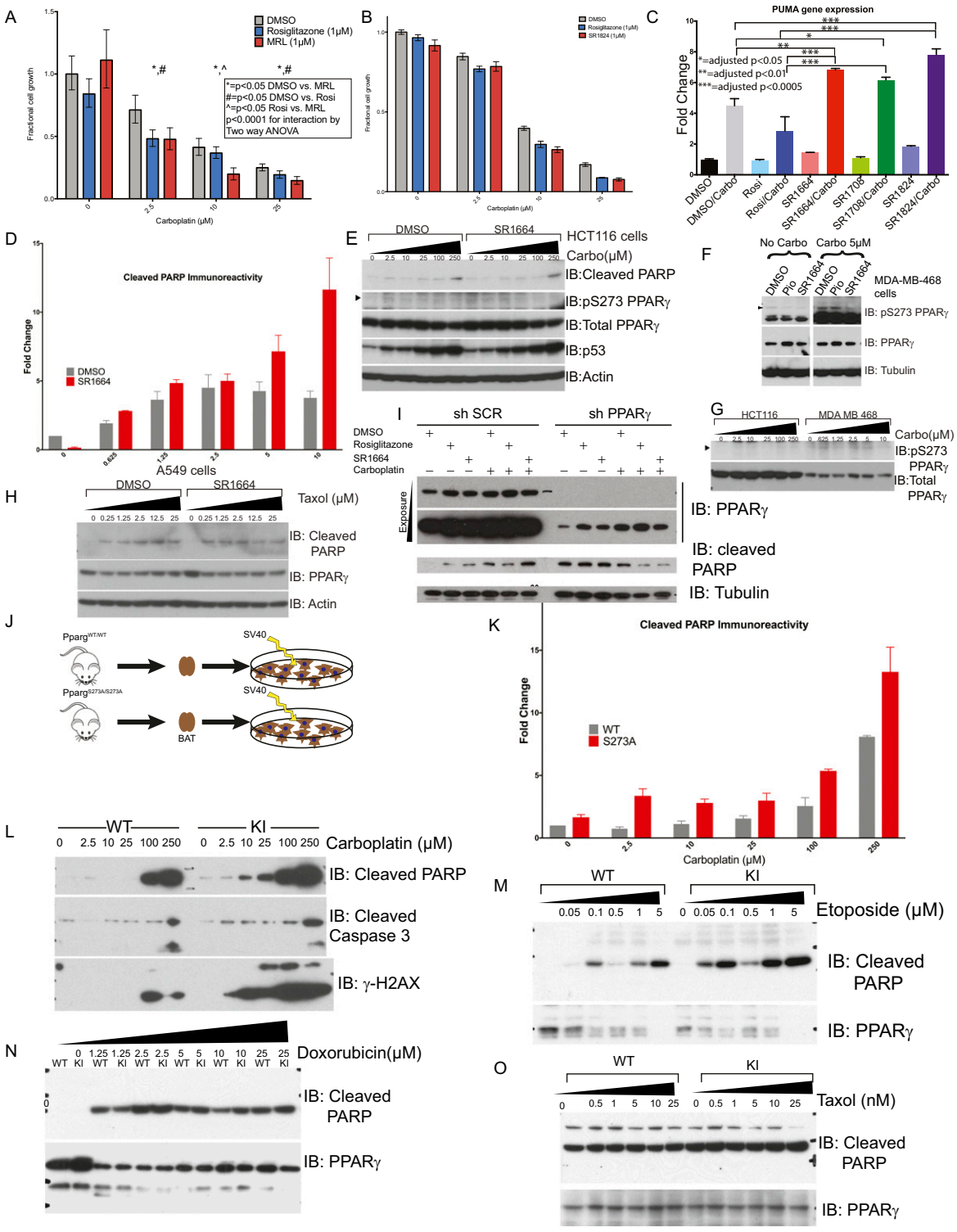

Fig. S1. (*A*) Treatment of A549 cells with other nonagonist PPARγ ligands with increasing concentrations shows similar effects on cell growth as rosiglitazone. The effect of MRL-24, a partial agonist, in combination with carboplatin is shown. There is a significant decrease in cell growth with cells treated with MRL-24 compared with all tested concentrations. (*B*) Cotreatment of A549 cells with SR1824, another noncanonical agonist ligand, with carboplatin also shows a sensitization effect at all concentrations tested. There was no difference in the effects of rosiglitazone and the nonagonist or partial agonist ligands. (*C*) Increase in PUMA gene expression with cotreatment of A549 cells with NALs. (*D*) Densitometric quantitation of cleaved PARP immunoreactivity of MDA-MB-468 cells treated in duplicate with SR1664 and carboplatin. Figures were analyzed in ImageJ and normalized to tubulin, then compared with the signal from the DMSO/untreated sample. Graph shows the mean ± SEM. (*E*) HCT116, a colorectal cancer line, are not sensitized to the effects of carboplatin by SR1664. There is no apparent increase in phosphorylation of PPARγ in this cell type, despite increases in accumulation of p53 in these cells upon treatment with carboplatin. (*F*) MDA-MB-468 cells also show phosphorylation of PPARγ on S273, which can be inhibited by the nonagonist ligand SR1664. Whole-cell lysates from cells were prepared after 24-h treatment with 5 μM carboplatin and cotreatment with the indicated drugs. Panels were from separate lanes of the same gel and blot. (*G*) Blot of pS273-PPARγ and total PPARγ from HCT116 cells (lanes 1–6) and MDA-MB-468 cells (lanes 7–12) treated with increasing concentration of carboplatin. Notably, the cells have difference IC50s for carboplatin, and thus different doses are used. HCT116 cells show minimal increase in phosphorylated PPARγ despite having significantly more total PPARγ than MDA-MB-468 cells. (*H*) A549 cells treated with paclitaxel and SR1664 do not show any increased apoptosis, in contrast to DNA damage directed chemotherapeutics. (*I*) Knockdown of PPARγ eliminates the sensitization of A549 cells to the combination of SR1664 and carboplatin. Cells infected with scrambled shRNA lentivirus continue to show increased PARP cleavage when treated with SR1664 and carboplatin. A lentiviral shRNA for PPARγ knocks down the protein level significantly (*Left* side), and abolishes the increase in cleaved PARP1 seen with the combination of SR1664 and carboplatin (*Right* side). (*J*) Schematic of our immortalization of fibroblasts generated from the brown adipose tissue (BAT) of mice bearing a homozygous knock in mutation of S273→A. (*K*) Densitometric quantitation of cleaved PARP immunoreactivity of BAT preadipocytes from wild-type or S273A KI genetic backgrounds treated in triplicate with increasing doses of carboplatin. Blots were analyzed in ImageJ and compared with the signal from the DMSO/untreated sample. Graph shows the mean ± SEM. (*L*) Treatment of fibroblasts derived from inguinal white adipose tissue (WAT) from wild-type and knock-in mice show a similar effect as those from BAT. Fibroblasts from inguinal WAT were isolated and immortalized using SV40 lentivirus. Wild-type and knock-in mutant fibroblasts were treated with increasing concentrations of carboplatin for 24 h. Whole-cell lysates were probed with the indicated antibodies. There was a significant increase in the accumulation of the markers of apoptosis, cleaved PARP1, and cleaved caspase 3. There was also increased accumulation of DNA damage, as evidenced by the increase in γ-H2AX. (*M*) Knock-in fibroblasts are more sensitive to the cytotoxic effects of etoposide, the topoisomerase II inhibitor. (*N*) These effects are also demonstrated with the anthracycline doxorubicin. (*O*) There is no apparent sensitization of S273A knock-in cells to the microtubule stabilizing chemotherapeutic paclitaxel.

1. Tontonoz P, Hu E, Spiegelman BM (1994) Stimulation of adipogenesis in fibroblasts by PPAR gamma 2, a lipid-activated transcription factor. *Cell* 79:1147–1156.
2. Lehmann JM, et al. (1995) An antidiabetic thiazolidinedione is a high affinity ligand for peroxisome proliferator-activated receptor gamma (PPAR gamma). *J Biol Chem* 270:12953–12956.
3. Kroll TG, et al. (2000) PAX8-PPARgamma1 fusion oncogene in human thyroid carcinoma [corrected]. *Science* 289:1357–1360; erratum in (2000) 289:1474.
4. Sarraf P, et al. (1999) Loss-of-function mutations in PPAR gamma associated with human colon cancer. *Mol Cell* 3:799–804.
5. Mueller E, et al. (1998) Terminal differentiation of human breast cancer through PPAR gamma. *Mol Cell* 1:465–470.
6. Mueller E, et al. (2000) Effects of ligand activation of peroxisome proliferator-activated receptor gamma in human prostate cancer. *Proc Natl Acad Sci USA* 97:10990–10995.
7. Smith MR, et al. (2004) Rosiglitazone versus placebo for men with prostate carcinoma and a rising serum prostate-specific antigen level after radical prostatectomy and/or radiation therapy. *Cancer* 101:1569–1574.
8. Burstein HJ, et al. (2003) Use of the peroxisome proliferator-activated receptor (PPAR) gamma ligand troglitazone as treatment for refractory breast cancer: A phase II study. *Breast Cancer Res Treat* 79:391–397.
9. Girnun GD, et al. (2008) Regression of drug-resistant lung cancer by the combination of rosiglitazone and carboplatin. *Clin Cancer Res* 14:6478–6486.
10. Girnun GD, et al. (2007) Synergy between PPARgamma ligands and platinum-based drugs in cancer. *Cancer Cell* 11:395–406.
11. Park J, Morley TS, Scherer PE (2013) Inhibition of endotrophin, a cleavage product of collagen VI, confers cisplatin sensitivity to tumours. *EMBO Mol Med* 5:935–948.
12. Soccio RE, Chen ER, Lazar MA (2014) Thiazolidinediones and the promise of insulin sensitization in type 2 diabetes. *Cell Metab* 20:573–591.

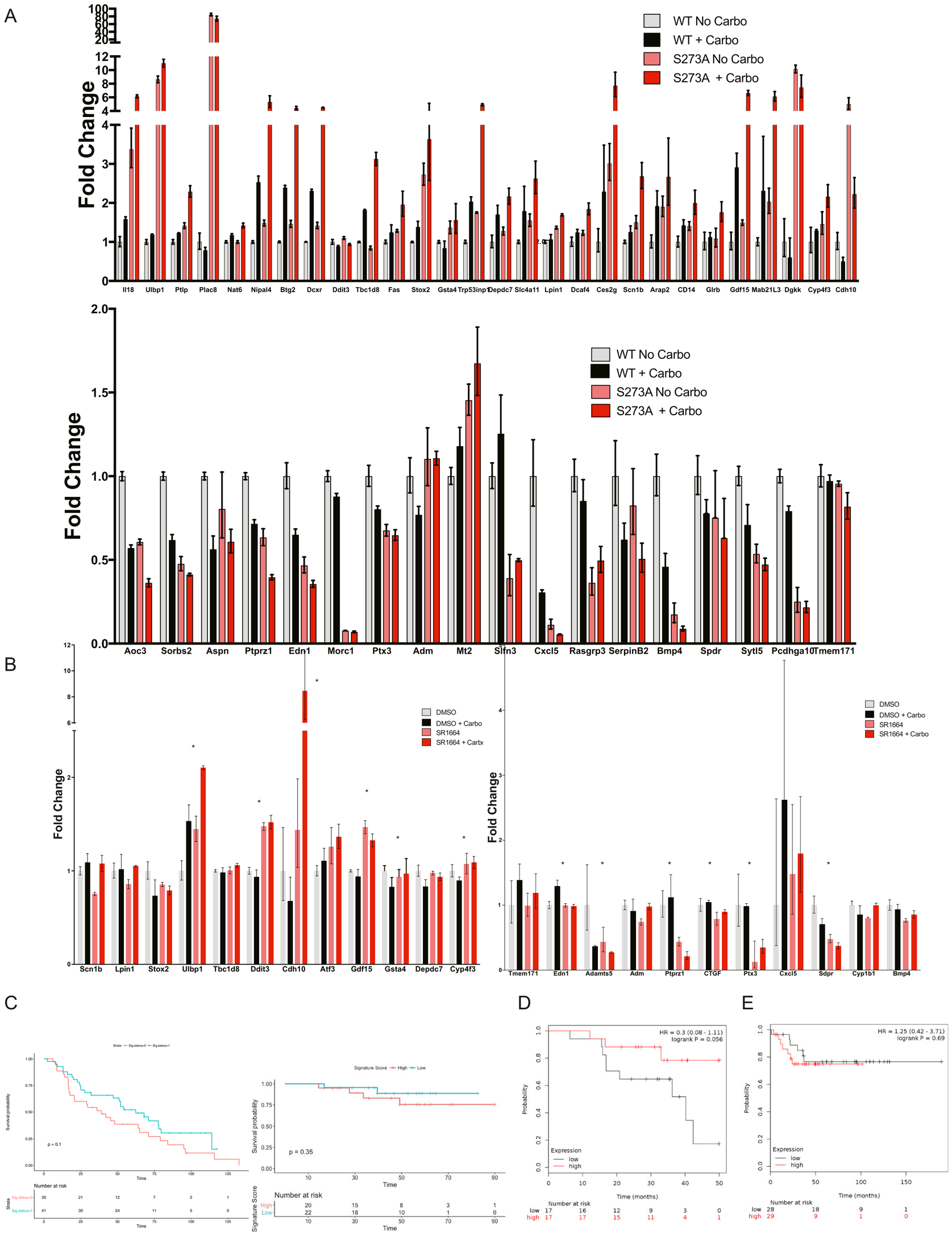

Fig. S2. (*A*) Validation of the genes most differentially expressed between wild-type and knock-in cells treated with carboplatin. Forty of 59 genes were appropriately regulated in the mutant cells treated with carboplatin compared with wild-type controls (χ^2 $P = 0.0063$). (*B*) MDA-MB-468 cells were treated with SR1664 and carboplatin or controls. RNA was harvested and analyzed by qPCR for the expression of the genes that are up-regulated in the core gene set of PPARγ phosphorylation inhibition. (*Right*) The same cells were analyzed for the core set of genes that are down-regulated upon inhibition of the phosphorylation of PPARγ and carboplatin treatment. *$P < 0.05$. (*C*) Separate analysis of the two cohorts pooled for Fig. 3*D*. For the Director's Challenge (*Left*) and the UT Lung Spore cohort (*Right*), a trend toward improved overall survival based on signature score was seen. (*D*) Kaplan–Meier analysis of ER^-/PR^- patients who did not receive chemotherapy using the KMplot online tool shows no difference in recurrence-free survival based on expression of the PPARγ S273A signature. (*E*) Kaplan–Meier analysis of overall survival of lung cancer patients using the KMplot online tool reveals a trend toward improved survival in patients with expression of the PPARγ S273A signature.

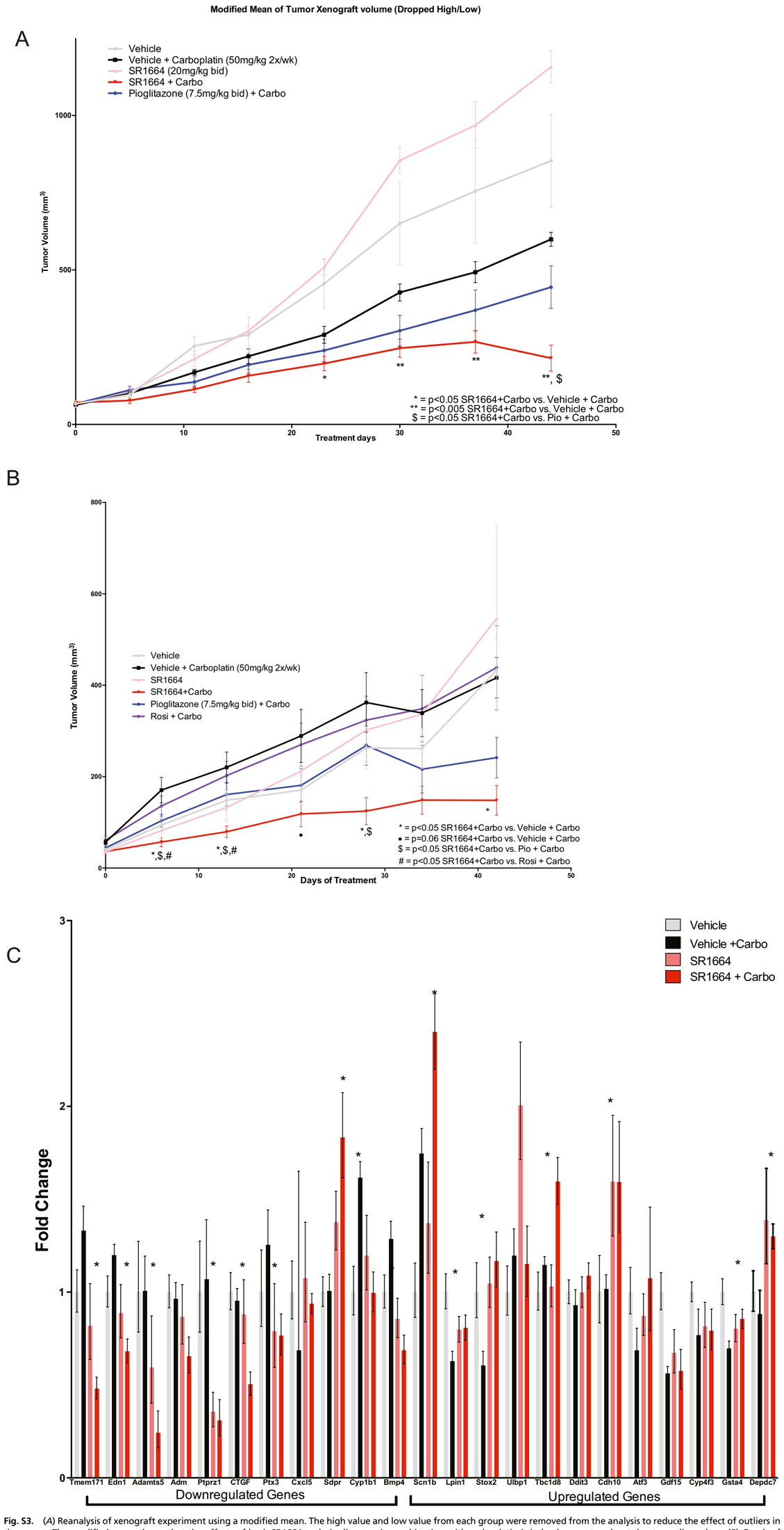

Fig. S3. (*A*) Reanalysis of xenograft experiment using a modified mean. The high value and low value from each group were removed from the analysis to reduce the effect of outliers in the group. The modified mean shows that the effects of both SR1664 and pioglitazone in combination with carboplatin is indeed present and not due to outlier values. (*B*) Graph of tumor volumes over time in a second independent experiment showing that SR1664 and carboplatin treatment is associated with a significantly lower volume compared with DMSO and carboplatin alone. (*C*) Analysis of the gene-expression set indicative of inhibition of PPARγ phosphorylation at S273 in the response to carboplatin suggests the efficacy of SR1664 and carboplatin treatment in the xenografts. Fifteen of 23 genes were regulated in the expected direction (*$P < 0.05$).

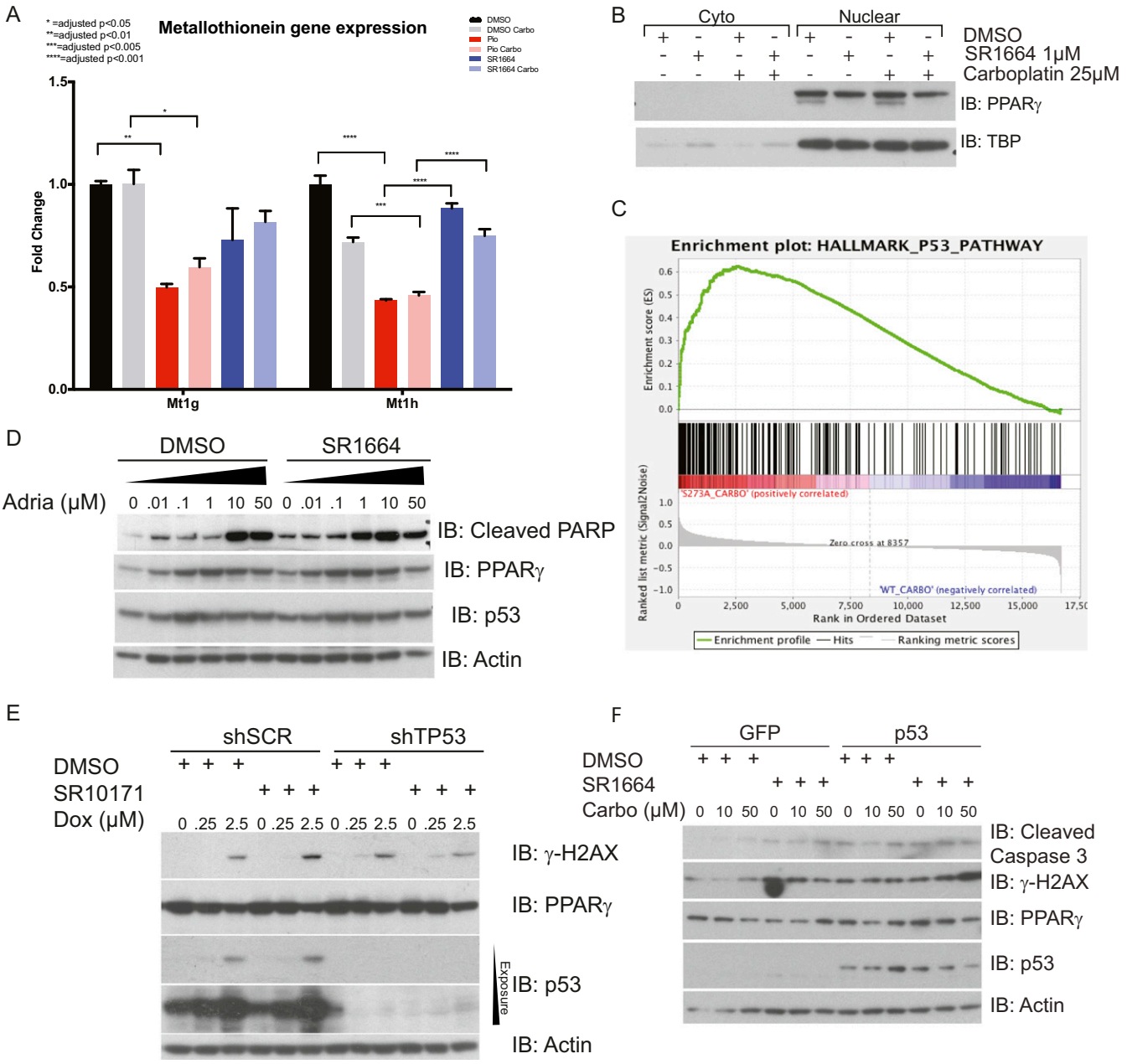

Fig. S4. (*A*) qPCR analysis of two of the metallothionein genes. Treatment of A549 cells with pioglitazone does reduce metallothionein gene expression. However, SR1664 has no effect on metallothionein gene expression, raising the possibility of an alternate mechanism of sensitization. (*B*) Nuclear extracts of A549 cells show no change in total PPARγ nuclear accumulation after treatment with carboplatin or SR1664. (*C*) The top scoring gene set from GSEA, which was enriched in the S273A fibroblasts, was the p53 pathway. (*D*) H2009 cells, which have a mutation in TP53 at codon 273, show no increase in DNA damage as measured by γ-H2AX staining or cell death upon cotreatment of nonagonist ligands and doxorubicin. (*E*) Lentivirally mediated shRNA mediated knockdown of p53 from A549 cells reveals increased sensitization to cytotoxic agents is dependent on p53. Compared with cells infected with a scrambled shRNA, cells with reduced accumulation of P53 due to a p53 shRNA show no increased γ-H2AX production when cells are treated with a nonagonist ligand and doxorubicin. (*F*) NALs do not sensitize p53 null Calu-1 cells to DNA damage from cytotoxic therapy, which can be rescued by reintroduction of wild-type P53.

Dataset S1. List of qPCR primers for PPARγ S273 gene sets

Dataset S1